Palaeohydrologic Estimates of Flood Discharge of Lower Ramganga River Catchment of Ganga Basin, India, Using Slackwater Deposits

3

Rameswar Mukherjee

Abstract

Conventional statistical methods for estimating recurrent intervals of the flood are less reliable due to the unavailability of recorded discharge data for a longer period. It can only be possible through palaeohydrological analysis along with sedimentological and geomorphic investigations. In the palaeohydrological study, palaeodischarge is calculated using slackwater deposits (SWD). These are the natural records of overbank megaflood deposits. In the present study, the SWD remain preserved in a natural levee section of the lower Ramganga river catchment wherein seven discrete megaflood events were identified. According to the calculated palaeodischarge stage (top elevation of each slackwater deposits layer), the palaeofloods events were reconstructed. The palaeodischarge of these floods was estimated which ranged from 2664.72 m^3/s to 4121.46 m^3/s. From recorded discharge data, the flood frequency was calculated by using Log Pearson type III distribution. The grain size analysis was carried out through the Malvern Mastersizer-S analyser. The slackwater deposits were differentiated clearly with slope clastic deposits by the grain size distribution.

Keywords

Palaeohydrology · Slackwater deposits · Palaeoflood events · Palaeostage · Discharge reconstruction

3.1 Introduction

Flood frequency analysis (FFA) using historical or gauging discharge records is considered as quite insufficient for the precise estimation of flood frequency and its magnitude. The longest gauging records (usually much less than 100 years) are also too short to provide trustworthy prediction for extreme flood events. Therefore, in order to understand the flood behaviour of any channel it is necessary to receive long-term records of the floods. It can only be possible from the sedimentary archives preserved in the flood plain region (Yang et al. 2000). The palaeoflood data provides long-term natural records of the flood histories (Baker 2008). By using this data, palaeoflood hydrological estimation can be made a long with sedimentological and geomorphological investigations. The flood frequency, magnitude and recurrent interval of mega floods spanned over the decades to thousands of years preserved as palaeoflood deposits can improve the FFA by

R. Mukherjee (✉)
Department of Geography, Samsi College, Samsi, Malda, West Bengal, India

© The Author(s), under exclusive license to Springer Nature Switzerland AG 2022

B. Pradhan et al. (eds.), *Spatial Modelling of Flood Risk and Flood Hazards*,
GIScience and Geo-environmental Modelling, https://doi.org/10.1007/978-3-030-94544-2_3

enhanced fitting of the probability functions (Webb et al. 1988; Thorndycraft et al. 2003; Benito et al. 2004).

The palaeoflood hydrology is the interdisciplinary science of reconstructing past flood events (Baker 1987, 2008). It plays an important role in the temporal analysis of flood and channel response to palaeoenvironmental change, planning for mitigation of flood hazard and protection of hydraulic engineering construction (Zha et al. 2009a, 2015; Zhou et al. 2016). According to Baker and Kochel (1988), *'Palaeoflood hydrology combines a multidisciplinary approach (stratigraphy, sedimentology, geomorphology and hydraulics) in the study of past or ancient floods, to decipher, quantitatively, past flood discharges, extending the record of extreme floods from centuries to thousands of years'*. Benito and Thorndycraft (2005) opined that in the palaeofloods study, the term palaeo has promoted to common fallacy that it is only used for estimating very old floods that occurred in the geological period. However, most of the palaeoflood hydrological analyses encompasses the study of prehistoric, historic or modern floods in ungauged basins. This study has been popularized widely around the world since the past four decades because of long-term natural records of high magnitude floods that provide better insight on the following issues: (i) risk assessment of extreme flood events; (ii) determination of extreme limit of flood magnitude; (iii) channel responses of flood in various hydroclimatic settings; (iv) assessing the sustainability of floodwater in dry climatic region (Knox 2000; Benito et al. 2003; Benito and Thorndycraft 2005; Baker 2006; Zha et al. 2009b).

The techniques for palaeohydrological analysis do not incorporate the direct measurement or observation of the flood. Instead, by applying numerous flood-induced marks on the landscape which are derived from channel features associated with floods or flood deposits, various indirect indices can be implied. These indices are applied to measure the palaeoflood, e.g., flood velocity, discharge and flood stage levels (Stokes et al. 2012). It is very useful for ungauged drainage systems or where the documentation of systematic records is short or not properly maintained.

Over the past four decades, the palaeoflood slackwater deposits (SWD) have been utilized as a robust tool for palaeohydrological research. This study has been successfully conducted in the United States (Baker 1983; Ely and Baker 1985; Enzel et al. 1994; O'connor et al. 1986, 1994; Wang and Leigh 2012; Greenbaum et al. 2014); Spain (Benito et al. 1998, 2003) China (Yang et al. 2000; Huang et al. 2012; Fan et al. 2015; Li et al. 2015; Zha et al. 2015; Mao et al. 2016) and in India (Kale et al. 1994, 1997, 2000, 2003, 2010; Sridhar 2007).

Although slackwater deposits are found in all climatic conditions at different geomorphic settings, most specifically its presence is marked in the arid and semi-arid region (Baker and Kochel 1988; O'Connor et al. 1994; Baker 2006). The rivers located in these regions are often experienced with very high rainfall for a short span of time. The heavy torrential rainfall generates a high flood situation, accompanied by heavy sediment load coming from the unconsolidated and uncovered sediment deposits (Hirschboeck 1988). During high flood situations, the sediment loads were deposited at or near the channel margin. These deposits were reworked by the channel with the passage of time. The rainfall, runoff, bioturbation, human and animal interference also cause damage to the primary sedimentary deposits. Apart from the arid and semi-arid regions, the SWDs are quite well preserved in the tropical region also (Ely et al. 1996; Kale et al. 2003, 2010; Kale 2008). It has been found that low to medium magnitude overbank flood deposits are more susceptible for undercutting and subsequent flow. Only the deposits of megaflood events remain in situ and probably preserved for a longer period (Ely et al. 1996).

According to Kale (2008), there is a low to moderately low chance of getting palaeoflood slackwater deposits in the Gangetic Plain region. This region is heavily populated and large-scale agricultural practices are going on since $\sim$5000 years near the river. Apart from that, the incidence of high magnitude flow causes frequent channel migration which brings inconsistencies in the successive records of flood deposits. In spite of such hindrances, if the researchers conduct a thorough field survey along the probable locations specifically in the Western Gangetic plain region, they may definitely get the well-preserved SWD data (Mukherjee 2019). The rivers located in the Western Gangetic plain region are incisional in nature and less dynamic than the Eastern Gangetic plain rivers (Sinha et al. 2005). In the incised channel, the flood deposits can be easily traced than the aggrading channel. Besides, there is a preponderance of partly confined channels in the western Gangetic plain region from where one can archive recurrent flood deposits. In the present study, palaeodischarge has been estimated on the lower Ramganga river, located in the Western Gangetic plain. The uncontrolled and unscientific growth of the human population in this river catchment has increasingly been posing the risk of flood on the human habitation as well as in the infrastructural development. Therefore, palaeoflood hydrological analysis can be fruitful for flood assessment, risk analysis, flood plain planning and management. The aims of the present study are as follows:

i. to describe and quantify extreme flood events using historical flood data;
ii. to discuss pedo-stratigraphic characteristics of palaeoflood slackwater deposits;
iii. to reconstruct extreme flood events using stratigraphic records of palaeoflood slackwater deposits;
iv. to estimate palaeoflood peak discharge by employing slope-area method.

3.2 Study Reach

The Ramganga river catchment is located in the Lesser and Outer Himalayas as well as in the Western Gangetic plain (Fig. 3.1). It drains an area of 30,635.1 km^2 (Mukherjee et al. 2017). The river originates from the Lesser Himalaya, near Gairsen, Uttarakhand. After flowing ∼167.91 km in the Himalayas, the Ramganga river debouches the Western Gangetic plain. The total length of this river is ∼649.11 km and it is a right-bank tributary of the Ganga river. The present study reach is located in Western Gangetic Plain locally known as *Rohilkhand Plain*. The study area is comprised of quaternary alluvium, namely: (i) Varanasi older alluvium (ii) Ramganga terrace alluvium and (iii) Ramganga recent alluvium, (Khan and Rawat 1992; Khan et al. 2016).

The Varanasi older alluvium is found in upland interfluves surface, sandy alluvial ridges, and older terrace surface (Fig. 3.2). The older and dissected terrace plain, inactive floodplains are composed by the Ramganga terrace alluvium and the Ramganga recent alluvium closely corresponds with active and younger floodplains (Mukherjee et al. 2017). The lower reach of the Ramganga river is unconstrained as a result of that frequent channel migrations are more common. The channel pattern alternates between meandering to partly braided types. At several places, high-curvature meandering channels are observed. The river is also characterized by higher stream power (Sinha et al. 2005; Mukherjee 2019). The fluvial regime of this river is largely controlled by the monsoon climate. This river catchment receives more than 80% of annual rainfall in the monsoon season (June to September). During this period, large floods are more common in the lower reaches of the catchment area (Fig. 3.3). Because of higher stream power, presence of easily erodable bank materials and fragile foundation of the natural levees, the floods become extremely hazardous in this study reach.

3.3 Database and Methodology

The present analysis has been done by using extreme flood discharge data and palaeoflood slackwater deposits (Fig. 3.4). The sources of data collection are given in Table 3.1.

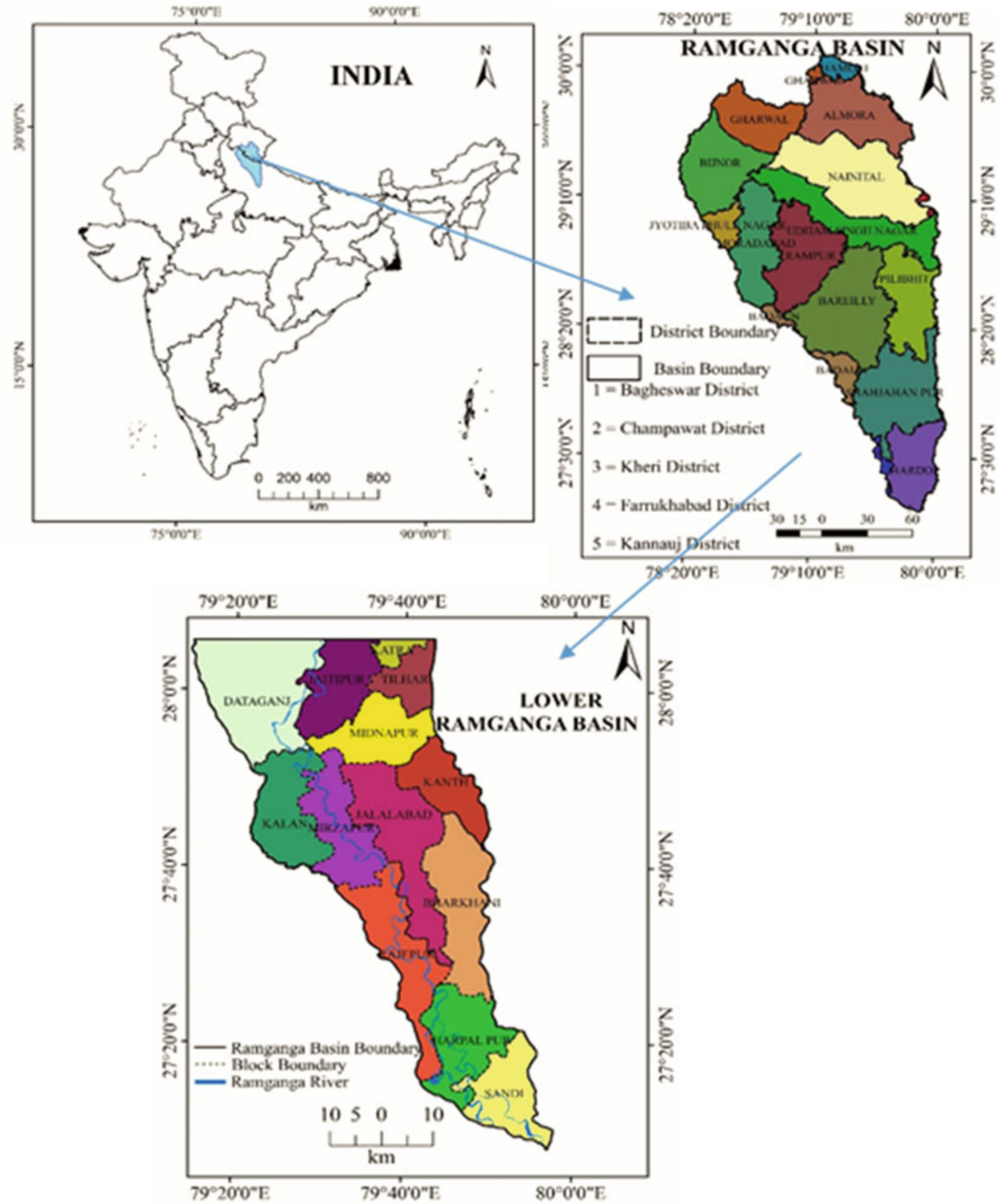

Fig. 3.1 Study reach

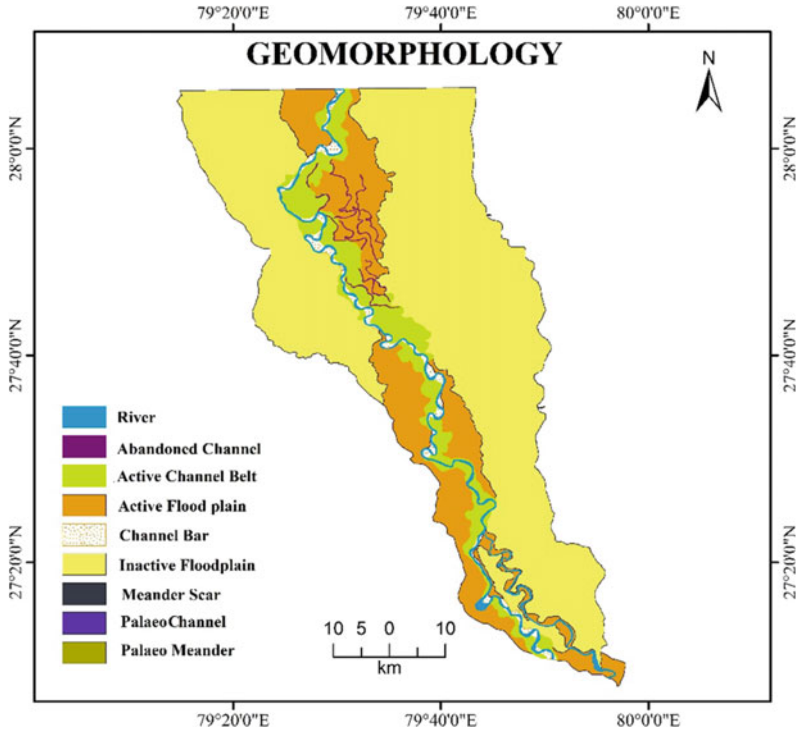

Fig. 3.2 Geomorphological map of the study reach

3.3.1 Flood Frequency Analysis by Log-Pearson Type III Distribution

For flood frequency analysis, the annual extreme discharge value was taken into consideration. The Log Pearson III distribution was used to estimate probable extreme flood frequencies of the Ramganga river. This measure is extensively applied for FFA to the major tropical rivers as it fits most appropriately to estimate flood peaks. This method involves first converting the variate into logarithmic form and then analyzing the transformed data (Subramanya 2013). Mukherjee and Bilas (2019) assessed the flood frequency of the lower Ramganga river by applying Gumbel's, Log-Pearson Type III, and Weibul's method, where it has been found that the Log-Pearson Type III is the most appropriate measure for FFA.

For calculating flood frequency of the lower Ramganga river by using Log-Pearson Type III distribution, the following steps were followed.

(i). At first, all the annual maximum flood discharge value was transformed into logarithms by using Eq. 3.1:

$$Y = logx \tag{3.1}$$

(ii). Then, the mean ($\bar{y}$), standard deviation ($\boldsymbol{\sigma_y}$), and skewness coefficient (C_s) of y series were estimated as

$$\bar{y} = \frac{1}{n}\sum y_i \tag{3.2}$$

$$\sigma_y = \sqrt{\sum(\boldsymbol{y} - \bar{\boldsymbol{y}})^2/(\boldsymbol{N}-\boldsymbol{1})} \tag{3.3}$$

$$C_s = \frac{\boldsymbol{N}\sum(\boldsymbol{y}-\bar{\boldsymbol{y}})^{\boldsymbol{3}}}{(\boldsymbol{N}-\boldsymbol{1})(\boldsymbol{N}-\boldsymbol{2})(\boldsymbol{\sigma_y})^{\boldsymbol{3}}} \tag{3.4}$$

(iii). The logarithms of extreme flood discharge were computed using the equation

$$5Y_T = \bar{y} + K_T\sigma_y \tag{3.5}$$

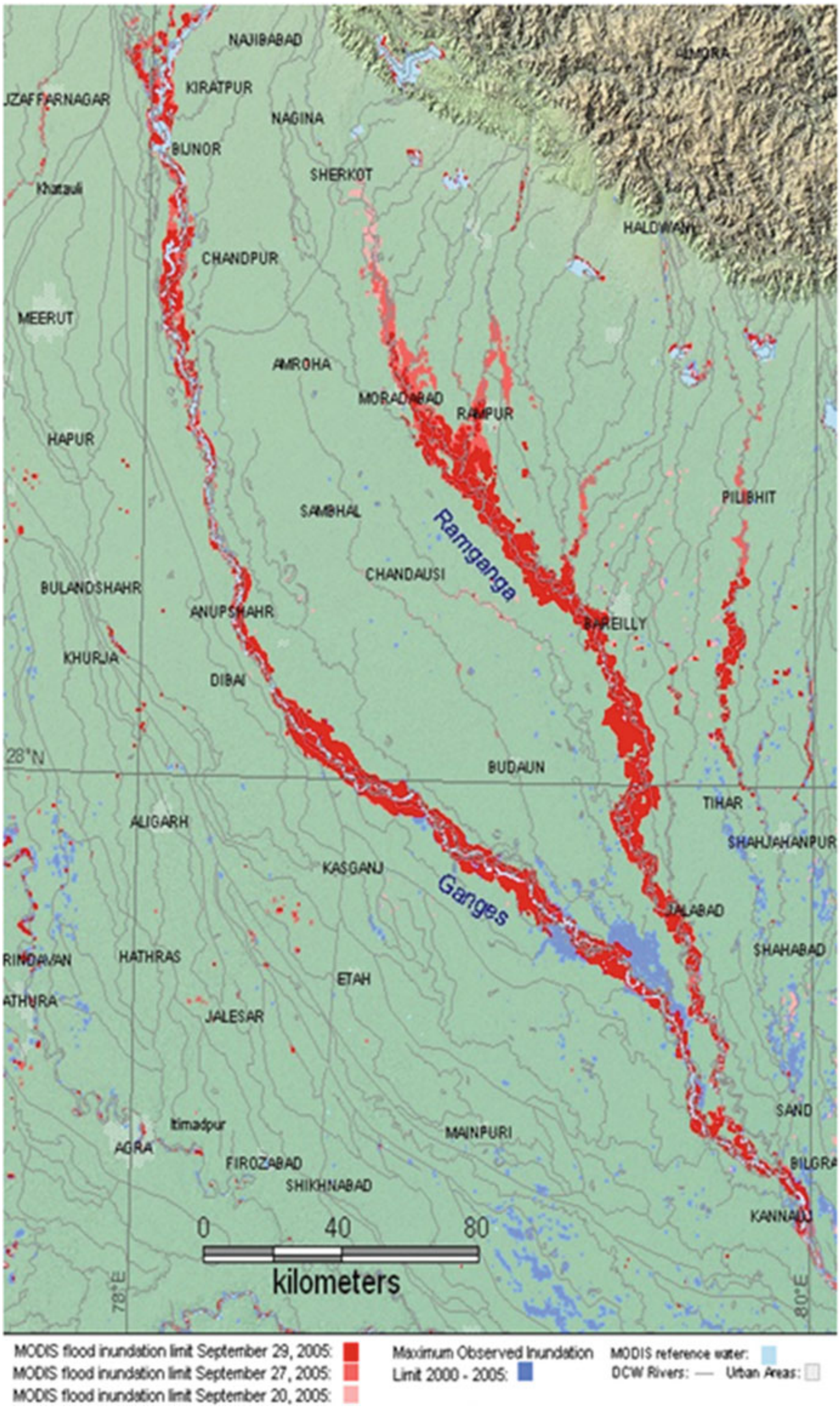

Fig. 3.3 Inundation map derived from MODIS Data (Dartmouth Flood Observatory 2014)

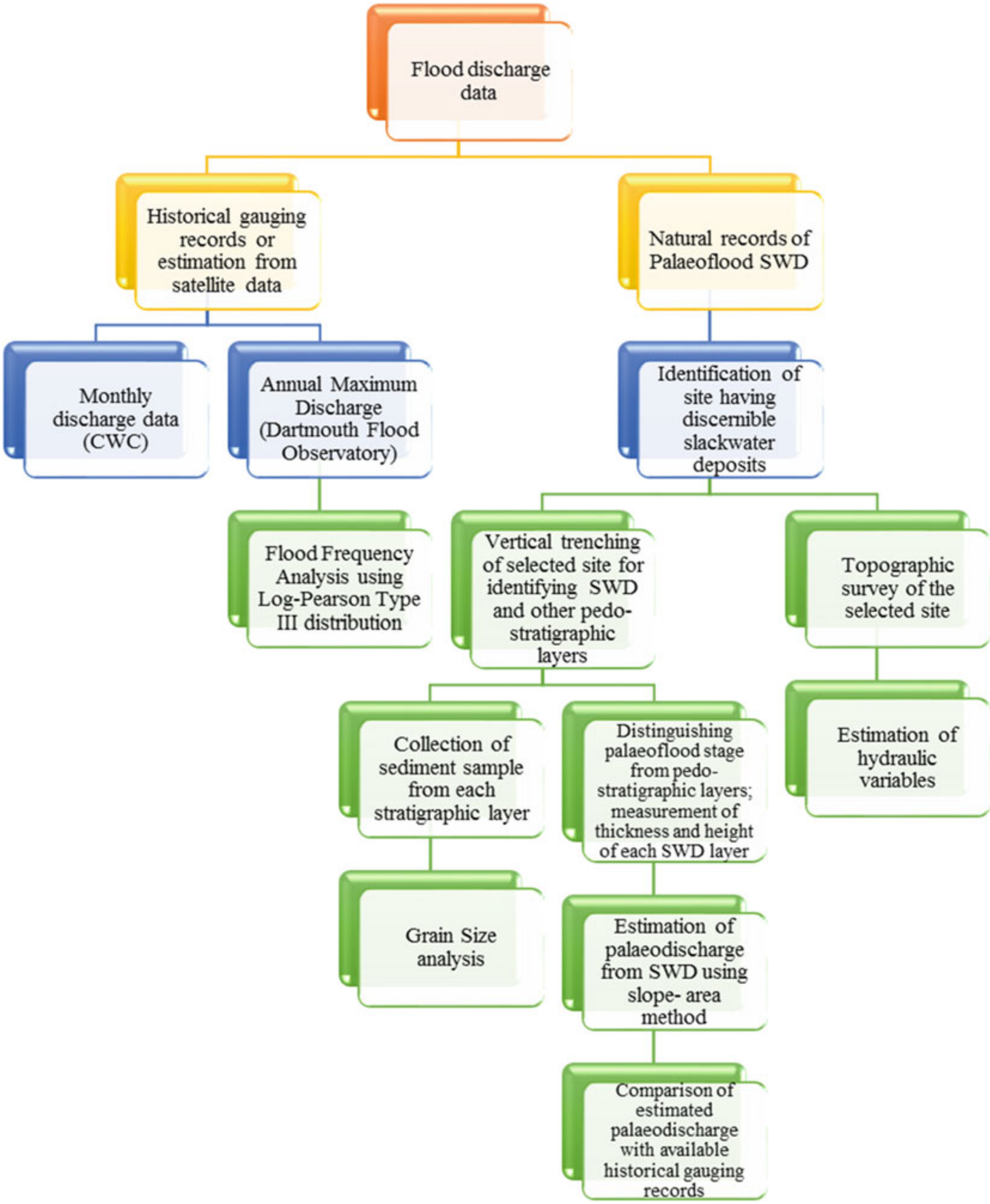

Fig. 3.4 Methodological Workflow

Table 3.1 Sources of data

Data types	Gauging site/survey site	Duration	Source
Maximum annual discharge	Dandi, Badaun District, UP	1998–2020	Dartmouth flood observatory Website (floodobservatory.colorado.edu)
Monthly annual discharge	Dabri, Shahjahanpur district, UP	1998–2002	Central Water Commission, Govt. of India
Slackwater deposit sample	Rampur Bajhera Village, Hordoi district, UP	20–26 March 2016	Personal Field Survey

The frequency factor K_T is a frequency factor that is a product of the return period and skewness coefficient

$$K_T = f(C_s, T) \quad (3.6)$$

(iv) After calculating y_T by Eq. (3.5), the extreme flood discharge value was obtained by antilogarithm of Y_T is

$$X_T = antilog(y_T) \quad (3.7)$$

3.3.2 Palaeoflood Hydrological Investigations

For palaeohydrological estimates of the lower Ramganga river, the methodological steps instructed by Benito and Thorndycraft (2005) were followed, which includes the following:

(i) For selecting suitable sites for palaeoflood slackwater deposits, a detailed study of topographical maps and satellite images of the lower Ramganga river catchment was carried out.
(ii) On the basis of that study, the most suitable sites of SWD were marked. A detailed field survey was conducted on those sites for identifying the presence of stratigraphic layers of slackwater deposits or other flood indicators.
(iii) The most prominent site was identified on a natural levee section where pedological and stratigraphic characteristics remain well preserved. The stratigraphic descriptions were made on the identified palaeoflood slackwater deposits.
(iv) The samples of flood deposits were collected for sedimentological analysis.
(v) A topographic survey was conducted on the selected SWD site and river reaches.
(vi) Estimation of hydraulic variables and palaeodischarge was carried out on the selected site.
(vii) A comparison was made with available historical or gauging records of the flood discharge
(viii) Flood frequency analysis was done.

In the present study, a geomorphic and sedimentological investigations were carried out in order to identify palaeoflood stage and estimate the frequency and magnitude of past megaflood events. In this study, the main objective of the fieldwork was to identify the palaeoflood stage (PFS). Then the PFS was converted into palaeoflood peak discharge. The reconstruction of PFS is dependent on the evolution, thickness, and attitude of the palaeoflood slackwater deposits (SWD) (Li et al. 2015). Basically, the top of the slackwater deposits can be extrapolated to estimate the PFS. Various river scientists used the elevation of the endpoints of palaeoflood SWD, which is in contact with the upper slope as PFS (Yang et al. 2000; Zha et al. 2009b; Wang et al. 2014).

The palaeodischarge was calculated by using slackwater deposits. These deposits were identified on the field based on several sedimentological criteria: (i) sediment deposits consisting silt, and silty-sand; (ii) abrupt vertical change in sediment grain size, colour, texture, and structure; (iii) clear division between successive stratigraphic layers; (iv) clay cap over the bed; (v) bioturbation which indicates exposure of sediment surface; (vi) existence of anthropogenic remains; (vii) presence of slope wash with angular clastic alluvial deposits between stratigraphic layers (Baker and Kochel 1988; Kale et al. 2000; Benito et al. 2003; Benito and Thorndycraft 2005; Thorndycraft et al. 2005; Sridhar 2007; Zhang et al. 2013, 2015).

After extensive field investigation, the most prominent SWD was found near Rampur Bajhera village in the Hardoi district of Uttar Pradesh (Fig. 3.5). Here a well-developed natural levee is present whose deposits did not get disturbed by burrowing animals or by anthropogenic activities. The natural levee Sect. (27° 29′26″, 79° 43′ 00″) has ~3.5 m elevation above the normal level of Ramganga. After observing the multi-temporal satellites and topographical maps it becomes evident that the region has remained relatively stable for the past 100 years. The stratigraphic records that remain preserved at the natural levee section were measured accurately. For palaeohydraulic investigation, the cross-section was measured in the field by using theodolite.

The palaeopeak discharge was reconstructed by using the slope area method of streamflow measurement (Manning, 1889). It was calculated as

$$Q = \frac{1}{n}(AR^{\frac{2}{3}}s^{\frac{1}{2}}) \tag{3.8}$$

where Q = Palaeoflood peak discharge (m^3/s),
n = Manning's n value or roughness value,
A = Cross-sectional area of the stream at the flood stage,
R = Hydraulic radius,
S = Water surface slope.

3.3.3 Grain Size Measurement

The sediment samples collected from a stratigraphic layer of the natural levee were measured using the Krumbein and Pettijohn (1938) standard pipette method. The size of the sand, silt and clay particles were measured using a Malvern Mastersizer-S analyser. But before that $CaCO_3$

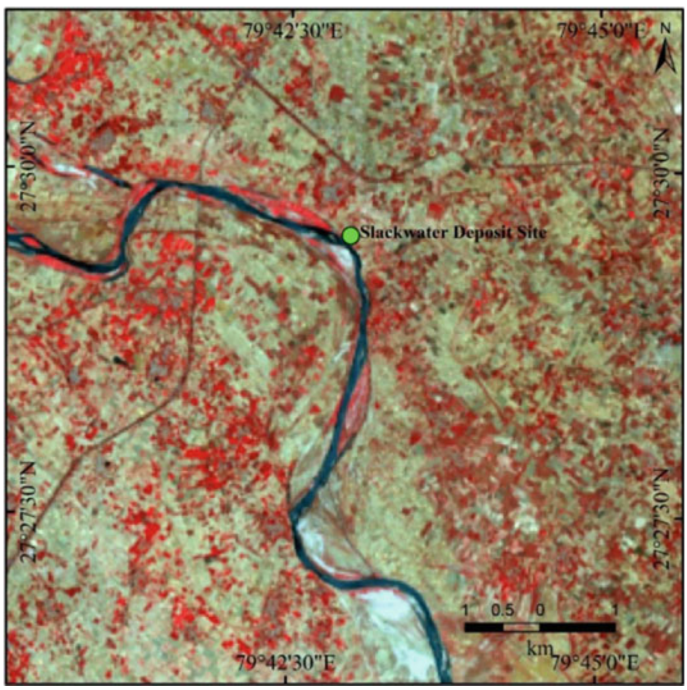

Fig. 3.5 Slackwater deposit Site (Natural Levee Section)

and organic matter contents were removed from the collected samples by providing pre-treatment with 10% HCl and 10% H_2O_2 solution.

3.4 Result and Discussion

3.4.1 Hydrological Characteristics

The Ramganga river is a spring-fed river and most of its tributary channels are either spring or groundwater fed. Hence, a majority of the water discharge of Ramganga and its tributary channels derives from the monsoon rainfall (Mukherjee and Bilas 2019). The monthly average discharge data (2003–2012) of Lower Ramganga river at Dabri gauging station (27° 53′ 1″ N and 79° 54′ 44″E) has been plotted in Fig. 3.6. It depicts the typical monsoon discharge of a river. It starts to rise from July and reaches a maximum in September and then declines from October. Every year, July to October is designated as the period of higher water discharge and it reaches an extreme level in August and September.

3.4.2 Estimation of Probable Flood Discharge and Flood Recurrence Interval

The flood frequency analysis is a statistical technique used to understand flood behaviour of any river. On the basis of that flood, forecasting can be made for a longer time period. This analysis involves the use of peak annual discharge to calculate probable flood discharge and its recurrent interval. The average of the observed peak discharge data is 1603.05 m^3/s and the standard deviation (SD) is 383.11 m^3/s. For Log-Pearson type III distribution, the mean and SD values of peak discharge are 3.193 and 0.105, respectively. For Log-Pearson III methods, frequency factor (K_T) has been used for measuring the peak flow. The calculation of various parameters for peak flow measurements at various recurrent intervals has been given in Table 3.2. It shows 2128.54 m^3/s for 10 years recurrent intervals, 2739.7 m^3/s for 100 years, and 3295.51 m^3/s for every 1000 years recurrent intervals.

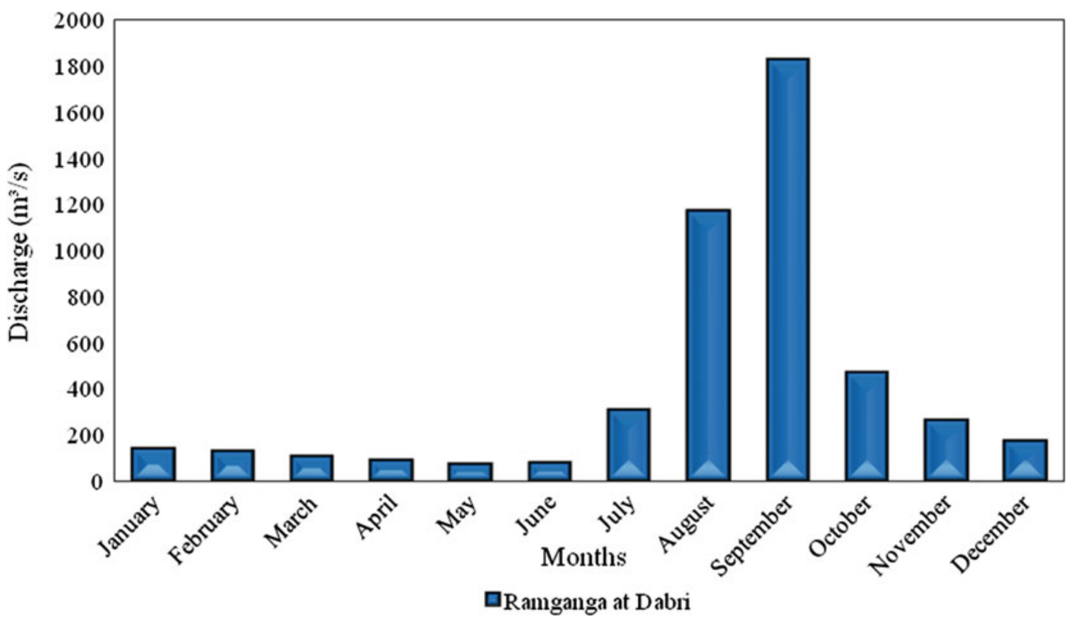

Fig. 3.6 Average monthly water discharge (2003–2012) of the Ramganga river at Dabri gauging station

Table 3.2 Calculation of probable peak discharge by using log-Pearson III method

Recurrent interval	Cs	K_T	y_T	x_T
5	0.48075	0.4852	3.243946	1753.66
10	1.282	1.2865	3.3280825	2128.54
20	1.595	1.5995	3.3609475	2295.87
25	1.751	1.7555	3.3773275	2384.12
50	2.054	2.0585	3.4091425	2565.34
100	2.326	2.3305	3.4377025	2739.7
200	2.576	2.5805	3.4639525	2910.42
500	2.769	2.7735	3.4842175	3049.42
1000	3.09	3.0945	3.5179225	3295.51

3.4.3 Estimation of Palaeohydraulic Flood Discharge Using Slack Water Deposits

For palaeoflood studies, the palaeodischarges of the basin have been calculated by marking the palaeostage indicators (PFS) (Baker et al. 1979). Flood exceeding a certain threshold has been registered through sedimentary records or other *'palaeostage indicators erosional landforms (stripped soils, flood scarps, high flow channels), and high-water marks (e.g., drift wood, tree impact scarps, silt lines)'* (Benito et al. 2003). The slackwater deposits (SWD) are formed by the material brought by flood and vertically accrete overbank. The top elevation of each slackwater deposit is considered as a palaeostage (Kochel and Baker 1982; Baker et al. 1983; Baker 1989). During the period of flood, fine-grained suspended sediments accumulate rapidly in a vertical sequence, where an abrupt drop of flow velocity occurs. When such a phenomenon occurs at the recurrent interval, a series of subsequent stratigraphic layers of slackwater deposits have been formed. These layers are generally separated by slope clastic deposits.

In the natural levee section, seven major palaeoflood events were recorded (Figs. 3.7 and 3.8). The PFS of each palaeoflood event was measured. Along with that, channel cross-sectional area, wetted perimeter, river gradient and hydraulic radius of the channel on both sections were measured most accurately. By using the slope-area method, the maximum palaeoflood discharge was estimated as 4121.46 m^3/s whereas the minimum value was recorded as 2664.72 m^3/s (Table 3.3).

3.4.4 Stratigraphy and Grain Size Analysis of Slackwater Deposits

In the natural levee section, total of 17 stratigraphic layers are observed. The pedo-stratigraphic descriptions have been given in Table 3.4. Out of which seven layers are designated as palaeoflood slackwater deposits. These layers are clearly visible and distinguishable from other layers. The colour of these deposits varies from yellow to orange. The concentration of silt to silty sand particles is higher, parallel to wavy laminations are found.

The grain size analysis was done in order to differentiate slackwater deposits from other sediments, to identify the proportion of sandy silt and clay deposits and also to distinguish the nature of their frequency distribution and degree of sorting. In the present stratigraphic section, all of the palaeoflood slackwater deposits are characterized by a higher degree of silty-sand concentration and they are well sorted (Table 3.5). The mean grain size of these deposits is ranged between 28.10 μm and 39.71 μm. The deposits of silty sand to coarse sand are predominantly higher in B2, B4 and D2 slackwater deposit layers. It demonstrates high energy flow and vertical accretion of the larger particles. The

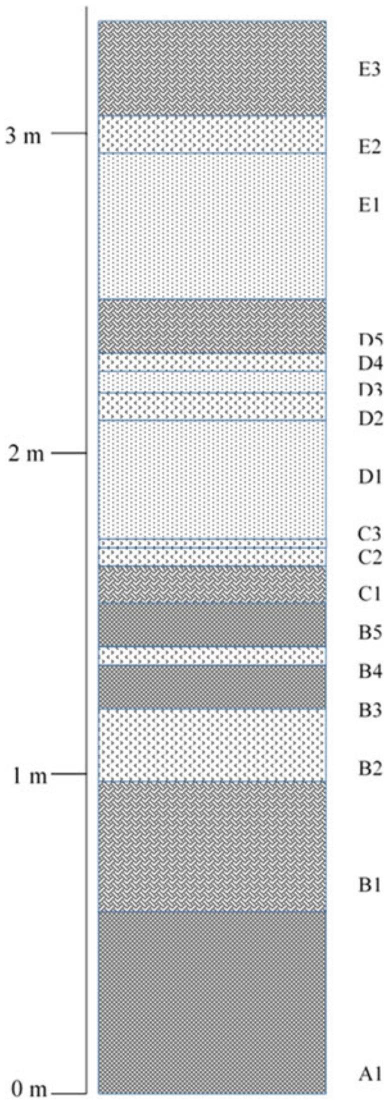

Fig. 3.7 Facies of natural levee section

Fig. 3.8 Natural levee section near Rampur Bajhera village, Hordoi district, UP (2016)

concentration of the coarser and unconsolidated materials is relatively higher in the upper stratigraphic section. The palaeosols are characterized by clay to clayey-silt deposits. On the other hand, in the recent soil deposits coarser silt and sand deposits predominate. The mean grain size increases in the upper section. The largest concentration of the clay and clayey-silt is found in the lowermost part of the stratigraphic section. Apart from that, the concentration of such materials is higher in B3, B5 and D3 layers,0 which are lying just above the layers of slack-water deposits. It depicts the period of low magnitude flood deposits. The values of kurtosis reveal that all of the deposits are characterized by platykurtic distribution. Its value increases in the upper layer deposits. All of the sediment distributions are positively skewed.

3.4.5 Accuracy Assessment

Based on present-day channel geometry and flood stage indicator the peak discharge of the 2011 megaflood has been estimated by applying the slope area method, i.e., 4396.81 m^3/s. The extreme flood discharge recorded as 4650.78 m^3/s in Dabri gauging site on 23 August 2011. On that day, the water level reached 138.515 m. It is

Table 3.3 Reconstructed peak discharges of the holocene paleofloods (Natural Levee Section)

SWD layer	Cross section area (m^2)	Wetted perimeter (m)	River gradient	Hydraulic radius (m)	Roughness coefficient	Palaeoflood peak discharge (m^3/s^{-1})
E2	5217.62	1534.8	0.0001	3.399	0.032	4121.46
D4	4713.75	1396.8	0.0001	3.375	0.032	3705.29
D2	4567.67	1318.1	0.0001	3.465	0.032	3654.48
C3	4478.23	1301.5	0.0001	3.441	0.032	3566.01
C2	4003.89	1280.9	0.0001	3.126	0.032	2990.7
B4	3964.95	1265	0.0001	3.134	0.032	2966.86
B2	3709.45	1258.2	0.0001	2.948	0.032	2664.72

Table 3.4 Pedo-stratigraphic description of natural levee section

Symbol	Pedo-stratigraphic Subdivision	Depth(cm)	Pedo-stratigraphic description
E3	Modern soil	0–030	Top soil, slope wash, granular soil structure, porous, upper part grass concentration is higher, abundant bio pores
E2	SWD	30–41.6	Palaeoflood slack water deposit, parallel lamination, yellow and light brown recent flood deposits
E1	Modern soil	41.6–87.4	Coarse to medium sand intermixed with silt, parallel to wavy lamination, high root density
D5	Modern soil	87.4–98.3	Slope wash deposits intermixed with coarse to medium sand and silt deposits parallel to the wavy lamination
D4	SWD	98.3–104.1	Slack water deposits, yellow-orange colour, parallel lamination, higher concentration of silty sand particles
D3	Modern soil	104.1–110.9	Parallel lamination sandy layer intermixed with silty layer
D2	SWD	110.9–119.6	Slack water deposits, yellow orange colour, silt to silty sand deposits
D1	Palaeosol	119.6–157.7	Sand deposits, medium to coarse size, white to light yellow colour, cross .bedding with climbing ripples, numerous silty lenses, presence of wavy lamination
C3	SWD	147.7–160.4	Palaeoflood slackwater deposits, parallel lamination, yellow to orange colour
C2	SWD	160.4–.167.25	Palaeoflood slack water deposits, lamination-cross lamination-pale to yellow-orangecolour, friable medium-grained sandy-silt
C1	Palaeosol	167.25–.178.1	Slope clastic deposits, medium to coarse-grained sand, unsorted, higher concentration of silty lenses, wavy lamination, high plant root density.
B5	Palaeosol	178.1–191.6	Clay layer dark grey, high plant root density
B4	SWD	191.6–197.5	Dull yellow-orange colour, soft silty-sands, parallel to wavy lamination bounded by clay layer in up and bottom
B3	Palaeosol	197.5–211.5	Dark clay layer-granular structure

(continued)

Table 3.4 (continued)

Symbol	Pedo-stratigraphic Subdivision	Depth(cm)	Pedo-stratigraphic description
B2	SWD	211.5–234.5	Slack water deposits, dominance of silt to silty clay, pale yellow orange colour, light brown medium grain sand in bottom and clay in top visible stratigraphic break, parallel to wavy lamination
B1	Palaeosol	234.5–275.5	Slope wash, sandy silt deposits, whitish to light yellowish colour, presence of plant roots, bears the deposits of low magnitude flood, higher concentration of silty lenses
A1	Palaeosol	275.5–332.5	Dark clay and clayey silt deposits predominate, grey to greyish brown color

Table 3.5 Particle-size distribution of the natural levee section

Symbol	Pedo-stratigraphic subdivision	Thickness (cm)	Grain Size (%)				Mean (μm)	Sorting	Skewness	Kurtosis
			<2 μm	2–16 μm	16–63 μm	>63 μm				
E3	Modern soil	30	6.98	34.3	39.10	19.62	44.32	0.29	1.05	1.12
E2	SWD	11.60	7.05	28.85	47.36	16.74	39.71	0.47	1.01	1.19
E1	Modern soil	45.8	10.1	31.4	40.7	17.80	47.51	0.30	0.89	0.98
D5	Modern soil	10.9	9.37	29.35	39.56	21.72	39.56	0.431	1.07	1.23
D4	SWD	5.8	6.59	27.81	42.93	22.67	46.74	0.28	0.81	0.91
D3	Modern soil	6.8	18.82	37.71	28.81	14.66	41.26	0.27	0.83	1.35
D2	SWD	8.7	7.26	26.05	43.59	23.1	37.89	0.23	0.77	0.83
D1	Palaeosol	38.1	13.48	26.73	38.71	21.08	50.73	0.39	1.08	1.01
C3	SWD	2.7	13.74	33.95	38.25	14.06	28.16	0.27	0.91	0.97
C2	SWD	6.85	11.84	37.21	35.73	15.22	29.4	0.20	0.99	0.64
C1	Palaeosol	10.85	8.09	32.06	42.79	17.06	39.88	0.29	0.87	0.74
B5	Palaeosol	13.5	19.09	38.16	31.50	11.25	30.47	0.26	1.02	0.93
B4	SWD	5.9	8.74	27.91	43.59	19.76	33.21	0.17	0.74	0.69
B3	Palaeosol	14.0	24.91	34.48	32.49	8.12	34.66	0.16	0.66	0.81
B2	SWD	23.0	10.8	32.75	41.87	14.58	28.10	0.18	0.48	0.59
B1	Palaeosol	41.0	18.21	36.93	35.26	9.60	29.89	0.31	0.63	0.71
A1	Palaeosol	57	37.33	40.81	20.7	1.16	22.85	0.14	0.55	0.57

considered that such magnitude of flood has never been experienced since the past 100 years (Mukherjee 2019). This gauging station of the lower Ramganga river, lying ~1.80 km upstream of the present surveyed section. The gauging record of extreme discharge of the 2011 flood closely corresponds to the present estimation.

3.5 Conclusion

The research on the palaeohydrological events has been carried out for temporal analysis of extreme flood behaviour in terms of its magnitude and recurrent interval and also to explain channel responses to such extreme floods in a particular reach of the river catchment. This kind of research might be very effective for floodplain planning and flood risk management, because if we know the extreme flood magnitudes, the flood inundation zone can be designated. On the basis of that long-term effective measures for flood adaptation and community resilience can be made. In the present paper, the magnitude and frequency of palaeofloods and historical flood events were reconstructed using palaeoflood slackwater deposits combined with a hydrographic survey, sedimentological analysis and instrumental records of floods.

The hydrological characteristics of the Ramgangariver are largely governed by the monsoon climate. For flood frequency analysis, annual peak discharge data has been used. To observe the chance of peak discharge of a certain magnitude of flood for lower Ramganga river Log-Pearson III distribution has been attempted. For 10–50 years of the recurrent interval of the flood, the peak discharge ranged from 2128.54 m^3/s to 2565.34 m^3/s for Log-Pearson III. Whereas for 100 years, it is estimated as 2739.70 m^3/s. A careful investigation for palaeoflood study was carried out in the alluvial reaches of the lower Ramganga in a ~3.5 m natural levee section (near Rampur Bajhera village, Hordoi district, UP). The study was based on identifying and marking Slack water deposits. On the basis of seven available SWD layers, palaeostage was measured on the field. By applying these palaeostage data, the palaeodischarges were extrapolated by using the slope-area method. The estimated palaeo peak discharge is ranged from 2664.72 m^3/s to 4121.46 m^3/s. The accuracy of the discharge estimation is dependent on the stability of the channel geometry over time. Such conditions may exist in stable bedrock confined channel reach. In the alluvial plain region, the instability of the channel is inherent, therefore, the possibility of uncertainty in the palaeodischarge may significantly arise. Although in the Western Gangetic plain region, partly confined channels are widely observed, where due to local resistance the river course remains stable over the period of time. If one can explore those places and trace out the palaeoflood deposits, the reconstruction of palaeohydraulic discharge and the time of flood occurrence would be possible. This kind of research will help to understand the nature and intensity of the past flood event accurately than the analysis of historical or gauging data. Hence, on the basis of palaeodischarge data, the future predictions can be made more efficiently.

References

Baker VR (1983) Palaeoflood hydrologic techniques for the extension of stream flow records. Transp Res Rec 922:18–23

Baker VR (1987) Palaeoflood hydrology and extraordinary flood events. J Hydrol 96:79–99

Baker VR (2006) Palaeoflood hydrology in a global context. CATENA 66:161–168. https://doi.org/10.1016/j.catena.2005.11.016

Baker VR (2008) Palaeoflood hydrology: origin, progress, prospects. Geomorphology 101:1–13

Baker VR, Kochel RC (1988). Flood sedimentation in bedrock fluvial systems. In Baker VR, Kochel RC, Patton PC (eds) Flood geomorphology. NY Wiley, pp 123–137

Baker VR, Kochel RC, Patton PC (1979) Long-term flood frequency analysis using geological data. The hydrology of areas of low precipitation. IAHS Publ 128:3–9

Benito G, Sopen´a, A., Sánchez-Moya Y, Machado MJ, Pérez-González A (2003) Palaeoflood record of the Tagus River (central Spain) during the late Pleistocene and Holocene. QuatSci Rev 22:1737–1756

Benito G, Thorndycraft VR (2005) Palaeoflood hydrology and its role in applied hydrological sciences. J Hydrol 313:3–15

Benito G, Lang M, Barriendos M, Llasat MC, Francés F, Ouarda T, Thorndycraft VR, Enzel Y, Bardossy A, Coeur D, Bobée B (2004) Use of systematic palaeoflood and historical data for the improvement of flood risk estimation: review of scientific methods. Nat Hazards 31:623–643

Benito G, Machado MJ, Perez-Gonzalez A, Sopena A (1998) Palaeoflood hydrology of the Tagus River, Central Spain. In Benito G, Baker VR, Gregory KJ (eds), Palaeohydrology and environmental change. Wiley: London, pp 317–333

Dartmouth Flood Observatory. Accessed on 01/02/2016 from http://www.dartmouth.edu/~floods/hydrography/E80N30.html

Ely LL, Baker VR (1985) Reconstructing Paleoflood hydrology with Slackwater deposits-Verde River, Arizona. Phys Geogr 6:103–126

Ely LL, Enzel Y, Baker VR, Kale VS, Mishra S (1996) Changes in the magnitude and frequency of late

Holocene monsoon floods on the Narmada River, central India. Geol Soc Amer Bull 108:1134–1148
Enzel Y, Ely LL, Martinez J, Vivian RG (1994) Paleofloods comparable in magnitude to the catastrophic 1989 dam failure flood on the Virgin River, Utah and Arizona. J Hydrol 153:291–317
Fan L, Huang CC, Pang J, Zha X, Zhou Y, Li X (2015) Sedimentary records of palaeofloods in the Wubu Reach along Jin-Shaan gorges of the middle Yellow River, China. Quatern Int 380–381:368–376
Greenbaum N, Harden TM, Baker VR, Weisheit J, Cline ML, Porat N, Halevi R, Dohrenwend J (2014) A 2000 year natural record of magnitudes and frequencies for the largest Upper Colorado River floods near Moab, Utah. Water Resour Res 50.https://doi.org/10.1002/2013WR014835
Hirschboeck KK (1988) Flood hydroclimatology. In: Baker VR, Kochel RC, Patton PC (Eds), Flood geomorphology. N.Y:Wiley, pp 27–49
Huang CC, Pang J, Zha X, Zhou Y, Su H, Zhang Y, Wang H, Gu H (2012) Holocene palaeoflood events recorded by slackwater deposits along the lower Jinghe River valley, middle Yellow River Basin. China. J Quat Sci 27(5):485–493
Kale VS (2008) Palaeoflood hydrology in the Indian context. J Geol Soc India 71:56–66
Kale VS, Achyuthan H, Jaiswal MK, Sengupta S (2010) Palaeoflood records from Upper Kaveri River, Southern India: Evidence for discrete floods during Holocene. Geochronometria 37:49–55
Kale VS, Mishra S, Baker VR (1997) A 2000-Year palaeoflood record from Sakarghat on Narmada, central India. J Geol Soc India 50:283–288
Kale VS, Singhvi AK, Mishra PK, Banerjee D (2000) Sedimentary records and luminescence chronology of late Holocene palaeofloods in the Luni River, Thar Desert, northwest India. CATENA 40:337–358
Kale VS, Ely LA, Enzel Y, Baker VR (1994) Geomorphic and hydrologic aspects of monsoon floods on the Narmada and Tapi Rivers in central India. Geomorphology 10:157–168
Kale VS, Mishra S, Baker VR (2003) Sedimentary records of palaeofloods in the bedrock gorges of the Tapi and Narmada Rivers, central India. Current Sci 84:1072–1079
Khan MYA, Daityari S, Chakrapani GJ (2016) Factors responsible for temporal and spatial variations in water and sediment discharge in Ramganga River, Ganga Basin. India. Environ Earth Sci 75:283
Khan AU, Rawat BP (1992) Quaternary geology and geomorphology of a part of Ganga basin in parts of Bareilly, Badaun, Shahjahanpur and Pilibhit district, Uttar Pradesh. Hyderabad: G.S.I
Knox JC (2000) Sensitivity of modern and Holocene floods to climate change. Quatern Sci Rev 19:439–457
Kochel RC, Baker VR (1982) Paleoflood hydrology. Science 215:353–361
Krumbein WC, Pettijohn FJ (1938) Manual of sedimentary petrography. Appleton Century-Crofts Inc., New York, pp 230–233
Li X, Huang CC, Pang J, Zha X, Ma Y (2015) Sedimentary and hydrological studies of the Holocene palaeofloods in the Shanxi-Shaanxi George of the middle Yellow River. China. Int J Earth Sci (geolrundsch) 104:277–288
Manning R (1889) On the flow of water in open channels and pipes. Trans InstCivEngIrel 20:161–207
Mao P, Pang J, Huang C, Zha X, Zhou Y, Guo Y, Zhou L (2016) A multi-index analysis of the extraordinary paleoflood events recorded by slackwater deposits in the Yunxi Reach of the upper Hanjiang River. China, Catena 145:1–14
Mukherjee R (2019) Ramganga River Basin- a geomorphological study of channel dynamics and palaeofloods, Unpublished PhD thesis, Dept. of Geography, Institute of Science, Banaras Hindu University, UP, India
Mukherjee R, Bilas R (2019) Flood frequency analysis of Ramganga River Basin in Western Gangetic Plain, India. NGJI Int Peer Rev J 65(3):286–299
Mukherjee R, Bilas R, Biswas SS, Pal R (2017) Bank erosion and accretion dynamics explored by GIS techniques in lower Ramganga river, Uttar Pradesh, India. Spatial Inform Res, 23-38.https://doi.org/10.1007/s41324-016-0074-2
O'Connor JE, Webb RH, Baker VR (1986) Palaeohydrology of pool-and-riffle pattern development: Boulder Creek. Utah, Geol Soc Amer Bull 97(4):410–420
O' Connor JE, Ely LL, Wohl EE, Stevens LE, Melis TS, Kale VS, Baker VR (1994) A 4500-year record of large floods on the Colorado river in the Grand Canyon, Arizona. J Geol 102:1–9
Sinha R, Jain V, Babu GP, Ghosh S (2005) Geomorphic characterization and diversity of the fluvial systems of the Gangetic Plains. Geomorphology 70(3–4):207–225
Sridhar A (2007) A mid–late Holocene flood record from the alluvial reach of the Mahi River, western India. CATENA 70:330–339
Stokes M, Griffiths JS, Mather A (2012) Palaeoflood estimates of Pleistocene coarse grained river terrace landforms (Río Almanzora, SE Spain). Geomorphology 149–150:11–26
Subramanya K (2013) Engineering hydrology. McGraw Hill Education (India) Private Limited: New Delhi
Thorndycraft VR, Benito G, Llasat MC, Barriendos M (2003) Palaeofloods, historical data and climatic variability: applications in flood risk assessment. In: Thorndycraft VR, Benito G, Barriendos M, Llasat MC (eds), Palaeofloods, historical data and climatic variability: applications in flood risk assessment. Madrid: CSIC, pp 3–9
Thorndycraft VR, Benito G, Rico M, Sopena A, Sanchez-Moya Y, Casa A (2005) A long-term flood discharge

record derived from slackwater flood deposits of the Llobregat River, NE Spain. J Hydrol 313:16–31

Wang L, Leigh DS (2012) Late-Holocene paleofloods in the Upper Little Tennesse River Valley, Southern Blue Ridge Mountains, USA. The Holocene 22(9):1061–1066

Wang L, Huang CC, Pang J, Zha X, Zhou Y (2014) Palaeofloods recorded by slackwater deposits in the upper reaches of the Hanjiang River valley, middle Yangtze River basin, China. J Hydrol 519:1249–1256

Webb R, O'Connor FE, Baker VR (1988) Paleohydroologic reconstruction of flood frequency on the Es' calante River. In Baker VR, Kochel RC, Patton PC (eds), Flood geomorphology: New York: John Wiley, pp 403–418

Yang D, Yu G, Xie Y, Zhan D, Li Z (2000) Sediment records of large Holocene floods from the middle reaches of the Yellow River, China. Geomorphology 33:73–88

Zha X, Huang C, Pang J (2009a) Palaeofloods recorded by slackwater deposits on the Qishuihe River in the Middle Yellow River. J Geog Sci 19(6):681–690

Zha X, Huang C, Pang J (2009b) Palaeofloods recorded by slackwater deposits on the Qishuihe River in the Middle Yellow River. J GeogrSci 19:681–690

Zha X, Huang C, Pang J, Liu J, Xue X (2015) Reconstructing the palaeoflood events from slackwater deposits in the upper reaches of Hanjiang River, China. Quatern Int 380–381:358–367

Zhang YZ, Huang CC, Pang JL, Zha XC, Zhou YL, Gu HL (2013) Holocene paleofloods related to climatic events in the upper reaches of the Hanjiang River valley, middle Yangtze River basin, China. Geomorphology 195:1–12

Zhang YZ, Huang CC, Pang JL, Zha XC, Zhou YL, Wang XQ (2015) Holocene palaeoflood events recorded by slackwater deposits along the middle Beiluohe River valley, middle Yellow River basin, China. Boreas 44:127–138. https://doi.org/10.1111/bor.12095.ISSN0300-9483

Zhou L, Huang CC, Zhou Y, Pang J, Zha X, Xu J, Zhang Y, Guo Y (2016) Late Pleistocene and Holocene extreme hydrological event records from slackwater flood deposits of the Ankang east reach in the upper Hanjiang River valley, China. Boreas. https://doi.org/10.1111/bor.12181